START-TO-END OPTIC OF THE FSF MULTI-TURN ERL PROJECT*

T. Atkinson[†], A. V. Bondarenko, A. N. Matveenko, Y. Petenev,
Helmholtz-Zentrum Berlin für Materialien und Energie GmbH (HZB), Germany

Abstract

Design studies for a future multi-turn ERL based light source at HZB are being investigated. The Femto-Science-Factory will provide its users with ultra-bright photons of angstrom wavelength at 6 GeV. The FSF is intended to be a multi-user facility and offer a wide variety of operation modes. A low emittance $\sim 0.1\,\mu$m rad mode will operate in conjunction with a short-pulse $\sim$10 fs mode. This paper reports on the full Start-to-End beam dynamic simulations for both modes.

INTRODUCTION

This paper continues on from a recent feasibility study [1] for Multi-turn ERL based light sources. The most recent additions to the optic are the vertical spreaders, the two stage injection process and a revised compression scheme.
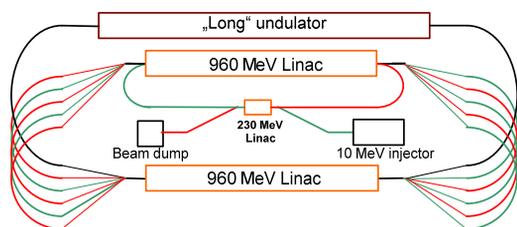

Figure 1: Schematic of the FSF Multi-Turn ERL.

Fig. 1 shows the layout of the light source. The difference in the two modes with regards to the lattice design occurs in the low energy section of the machine. For the Low Emittance Mode (LEM) a beam of higher charge is accelerated on crest in all of the linacs and circulates round isochronous Arcs. The Short Pulse Mode (SPM) however relies on achromatic arcs for the telescopic compression technique removing the correlated energy spread due to the off-crest acceleration. The modes share common High Energy Arcs where radiation effects play an important role in emittance growth.

VERTICAL SPREADERS

Optic of the vertical spreaders for all energies are the most recent elements to be integrated allowing the full Start-to-End beam dynamic simulations discussed in this paper. The geometry has been designed so that the total length of the structure is restricted to 25 m. Magnets are shared between energies when separation is no longer possible. The optic

is isochronous, contains sextupoles to correct the second order for high energy spread beams, and the beta functions are minimized throughout. Due to these heavy demands, the 4 and 6 GeV spreaders bend in both transversal planes and solenoids are implemented to correct the rotation of the coupled betatron oscillation. The design of the vertical spreaders is such that if the energy is changed, due to possible upgrades or unforeseen circumstances one would simply scale the field gradient in the magnets with that in the cavity rather than modify the complicated spreader geometry.

TWO STAGE INJECTION

Table 1 shows a subtle beam transformation through the space charge dominated injection process to produce a low emittance beam in all dimensions. These ASTRA [2] beam distributions are then converted, matched and tracked onwards using Elegant [3].

Table 1: Injector ASTRA Simulations 15pC LEM

Pos.	ε_{nx} (mm mrad)	ε_{ny} (mm mrad)	Ss (mm)	Energy (MeV)
Gun	0.27	0.27	2.50	1.91
Booster	0.22	0.22	2.38	9.45
Merger	0.19	0.16	0.95	9.45
Injection Linac	0.13	0.09	0.93	53.41

Producing a femto-second low energy spread pulse requires compression wherever feasibly possible. Here in the 1st part of the two stage injection scheme the longitudinal electron beam properties, Table 2, are restricted by the photo-injector laser pulse and the superconducting RF acceleration.

Table 2: Injector ASTRA Simulations 5pC SPM

Pos.	ε_z (keV mm)	Ss (mm)	Energy (MeV)
Gun	11.05	2.37	1.90
Booster	0.84	2.23	9.47
Merger	1.11	0.63	9.47
Injection Linac	2.36	0.60	53.41

A 3rd harmonic cavity is then used to linearize the longitudinal phase space [4] and lower the emittance. Subtle compression in the Merger between the Booster and finally the 1st cyromodule in the injection linac is required to minimize transversal emittance growth due to space charge effects.

05 Beam Dynamics and Electromagnetic Fields

D01 Beam Optics - Lattices, Correction Schemes, Transport

The 2nd part of the two stage injection scheme uses an injector Linac and Arc to prepare the beam for the main accelerator. The combination of off-crest acceleration in the linac and the R56 in the Arc further compress the beam from 2 to 1 ps.

LOW EMITTANCE MODE

The transverse emittance growth is kept to a minimum throughout the whole 8 km machine, Fig. 2 to utilize the undulator radiation in all acceleration and deceleration sections in order to maximize user potential. Plotted is both the horizontal (black) and vertical (red) normalized emittance.
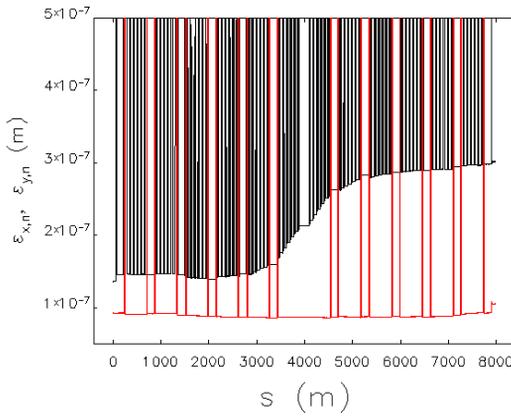

Figure 2: Start-to-end emittance plot for the LEM.

Plotted is the emittance including the dispersive contribution, seen in black as numerous peaks in the horizontal arcs, and red only in the vertical spreaders. The High Energy Arcs are designed to manipulate the horizontal phase advance to eliminate (in the 1D case) unwanted CSR induced emittance growth [5]. For a system of N identical isochronous bends, the CSR shift is given by Eq. 1.

$$\begin{pmatrix} \delta x \\ \delta x' \end{pmatrix}_N = \left(I \sum_{n=0}^{N} cos(n\mu_x) + J \sum_{n=0}^{N} sin(n\mu_x) \right) \begin{pmatrix} \delta x \\ \delta x' \end{pmatrix}_0 \quad (1)$$

If $\mu_x = 2\pi \cdot k/N$ where k is an integer, the impact of CSR on the transversal emittance is nullified [6]. Fig. 3 shows the twiss-functions for two (of six) $30\,°$ cells of the High Energy Arc each with a horizontal phase advance $\mu_x = 2\pi \cdot 3/4$.

There are four quadrupoles at the beginning and end of each cell to match the twiss parameters to those needed for the undulator sections between the Arcs. Triplets are used in the undulator section to further focus the beam in both planes about $\beta_{xy} \sim 10$ m and the bending cells are isochronous.

For the low emittance mode Fig. 2, with all the suppression techniques described in place, the transversal emittance mainly grows due to radiation effects and can be analytically estimated in the 6 GeV arc, using the radiation integral to cross reference the plotted emittance growth by simply using Eq. 2 [7].

$$\gamma\Delta\varepsilon \simeq 4 \cdot 10^{-8} E^6 I_5 = 0.04 \text{ mm mrad} \quad (2)$$
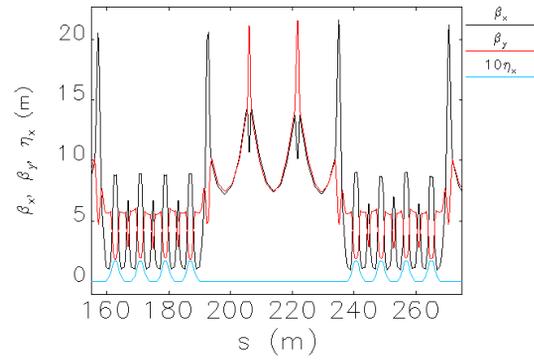

Figure 3: Twiss functions of a bend-undulator-bend section.

Table 3 summarizes the main beam dynamic parameters at various stages across the machine, (minimal emittance).

Table 3: Start-to-End LEM 15pC

Pos	ε_{nx} (mm mrad)	ε_{ny} (mm mrad)	St (ps)	$\Delta E/E$ (10^{-3})	Energy (MeV)
Input	0.14	0.09	3.09	2.93	50
Undulator	0.21	0.09	2.71	0.26	6000
Output	0.30	0.11	3.09	14.51	50

The 1.5 % output energy spread is foreseen as unproblematic for the future beam dump design. Symmetric to the injection process, the beam will then be further decelerated to 10 MeV and dumped.

SHORT PULSE MODE

Each off-crest acceleration followed by achromatic Arcs constitute the telescopic compression scheme in the lower energy acceleration sections. The first two Arcs up to a beam energy of 2 GeV have $\phi_1 = +10\,°$, $\phi_2 = -19\,°$ and positive $R56_1 = 20$ cm and $R56_2 = 8$ cm values. On recovery the linac phase is shifted $\phi_{1,2} \to \phi_{1,2} + 180\,°$ (ERL process) and the Arcs have the corresponding symmetric negative $R56$ values.

The longitudinal emittance compensation scheme uses the higher order magnetic terms created in the Arc and the off-crest acceleration Eq. 3 to recover the longitudinal emittance of the injector.

$$\epsilon_z^2 = < (c\Delta t_2)^2 >< \delta_2^2 > - < (c\Delta t_2 \delta_2) >^2 \quad (3)$$
$$\epsilon_z^2 = (T_{566} R_{65}^3 - T_{655})^2 < (c\Delta t_0)^4 >< (c\Delta t_0)^2 >$$

The accelerating phase ϕ determines both the R65 and T655 terms and sextupoles in the Arc+Spreader can adjust T566 to compensate longitudinal emittance growth.

Fig. 4 shows the recovery of normalized longitudinal emittance (black) using sextupoles in the first two Arcs with the optimum T_{566} for the given linac phase. The longitudinal

05 Beam Dynamics and Electromagnetic Fields

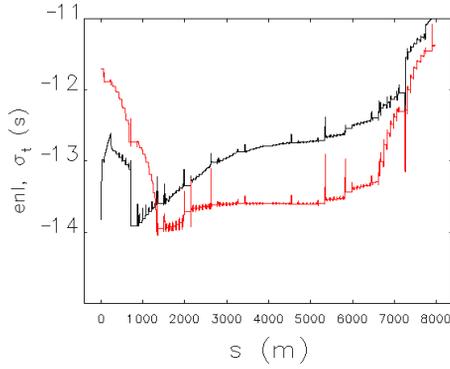**D01 Beam Optics - Lattices, Correction Schemes, Transport**
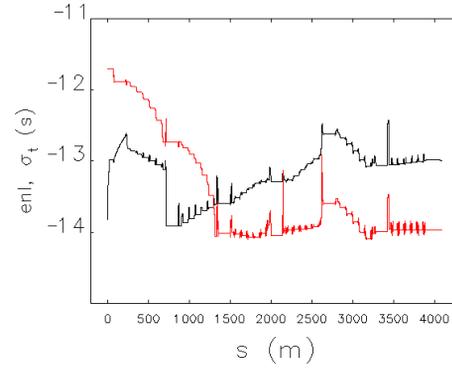
Figure 4: Log plot of the longitudinal bunch properties.

Figure 5: Selective bunch lengths using high order magnets.

emittance then starts to increase (s > 0.75 km) due to the coherent radiation effects associated with short bunches, producing the unwanted energy spread. Shown also is the bunch length (red) along the whole machine. The logarithmic plot (where -14→10 fs), shows an optic producing a bunch length of less then 10 fs for 2-3 GeV then approximately 25 fs at the long undulator section at the half way point along the machine.

The 3 stage compression scheme using the second part of the injection process and the circulation about the two 1 GeV linacs have different a phase sensitivities. Simulation results given in Table 4 can be varified analytically by finding the root of the product of its longitudinal transfer matrix, Eq. 4

$$\begin{pmatrix} c\Delta t \\ \delta \end{pmatrix}_{\text{end}} - \prod_{i,j=1}^{3} M_{\phi_i} M_{\text{ARC}_j} \begin{pmatrix} c\Delta t \\ \delta \end{pmatrix}_{\text{start}} == 0 \qquad (4)$$

given

$$M_{\phi_i} = \begin{pmatrix} 1 & 0 \\ -\frac{U\omega}{cE_2}\sin(\phi_i + d\phi) & \frac{E_1}{E_2} \end{pmatrix}, \quad M_{\text{ARC}_j} = \begin{pmatrix} 1 & R56_j \\ 0 & 1 \end{pmatrix}$$

The figure of merit of the sensitivity is the phase shift $d\phi$ in a given linac required to double the final bunch length $c\Delta t_{\text{end}} = 8 \to 16$ fs at 2 GeV (s = 1250 m in Fig. 4).

Table 4: Phase Sensitivity of the 3 Stage Compression

Pos.	ϕ_i (°)	$d\phi_{\text{sim}}$ (°)	$d\phi_{\text{root}}$ (°)
Injection	2.90	0.15	0.16
Linac1	10.45	0.10	0.07
Linac2	-19.00	3.50	3.28

One can apply additional longitudinal gymnastics Fig. 5 in the High Energy Arcs to obtain 10 fs at 6 GeV. Here the sextupoles are optimized so that the increase in bunch length due to the horizontal part of the 4 GeV vertical spreader (step at s = 2500 m) is re-compressed using higher order terms described in Eq. 3 to replenish the 10 fs project goal for high peak brightness in the 6 GeV long undulator.

However the inclusion of such high order magnets has a negative impact on the transversal emittance and realistic recovery is not possible using the present spreader optic, which are common to both operation modes, therefore a compromise is necessary.

Table 5: Start-to-End SPM 5 pC

Pos	ε_{nx} (mm mrad)	ε_{ny} (mm mrad)	St (fs)	$\Delta E/E$ (10^{-3})	Energy (MeV)
Input	0.11	0.06	2002	0.48	50
Undulator	0.35	0.11	25.29	0.56	6000
Output	7.32	11.09	4182	29.40	50

The bunch length on recovery compared to injection in Table 5 has doubled. This is again instigated as a compromise to relax the transversal plane parameters in the final few critical sections of the machine.

REFERENCES

[1] T. Atkinson et al., "Start-to-end Beam Dynamics simulations for Femto-Science-Factory Feasibility Study", ERL2013, Novosibirsk.

[2] ASTRA code, A Space Charge Tracking Algorithm, http://tesla.desy.de/ meykopff/ 2012.

[3] M. Borland, "elegant: A Flexible SDDS-Compliant Code for Accelerator Simulation", Advanced Photon Source LS-287, September 2000.

[4] A. N. Matveenko et al, "Multi-turn ERL-based Synchrotron Light Facility: Injector Design", IPAC14, MOPRO107.

[5] J. Wu et al., PAC 2001, p.2866-2868.

[6] A. V. Bondarenko et al, "Suppression Techniques of CSR Induced Emittance Growth in ERL Arcs", IPAC14, TUPRO037.

[7] D. Angal-Kalinin, "Emittance growth due to incoherent synchrotron radiation", 2nd CLIC Workshop, CERN 2008.

05 Beam Dynamics and Electromagnetic Fields

D01 Beam Optics - Lattices, Correction Schemes, Transport